ACS APPLIED MATERIALS & INTERFACES

Research Article

www.acsami.org

Step Terrace Tuned Anisotropic Transport Properties of Highly Epitaxial $LaBaCo_2O_{5.5+\delta}$ Thin Films on Vicinal $SrTiO_3$ Substrates

Q. Zou,[†,⊥] M. Liu,[‡,⊥] G. Q. Wang,[†] H. L. Lu,[†] T. Z. Yang,[†] H. M. Guo,*[,†] C. R. Ma,[‡] X. Xu,[‡] M. H. Zhang,[§] J. C. Jiang,[§] E. I. Meletis,[§] Y. Lin,[∥] H. J. Gao,[†] and C. L. Chen*[,‡]

[†]Institute of Physics, Chinese Academy of Sciences, Beijing 100080, China

[‡]Department of Physics and Astronomy, University of Texas at San Antonio, San Antonio, Texas 78249, United States

[§]Department of Materials Science and Engineering, University of Texas at Arlington, Arlington, Texas 76019, United States

[∥]State Key Laboratory of Electronic Thin Films and Integrated Devices, University of Electronic Science and Technology of China, Chengdu, Sichuan 610054, P. R. China

Supporting Information

ABSTRACT: Highly epitaxial $LaBaCo_2O_{5.5+\delta}$ (LBCO) thin films were grown on different miscut (001) $SrTiO_3$ substrates (miscut angle of 0.5°, 3.0°, and 5.0°) to study the substrate surface step terrace effect on the in-plane electrical transport properties. The microstructure studies by X-ray diffraction and transmission electron microscopy indicate that the as-grown films are A-site disordered cubic perovskite structures with the *c*-axis highly oriented along the film growth direction. The four-probe scanning tunneling microscopy (STM) studies show that the LBCO thin films grown on the vicinal $SrTiO_3$ substrates have a typical semiconductor behavior with the substrate surface terrace step inducing anisotropic electronic transport properties. These results indicate that in highly epitaxial thin films the surface terrace step induced local strains can play an important role in controlling the electronic transport properties and the anisotropic nature.

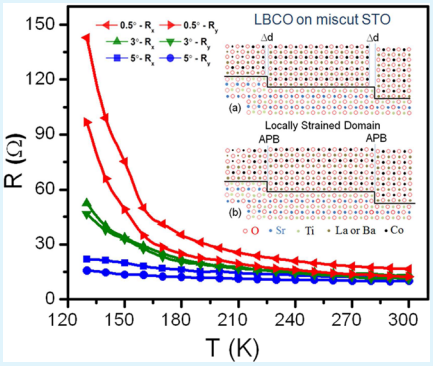

KEYWORDS: *LBCO, STO, miscut substrate, step terrace induced strain, anisotropic properties, small polaron*

Perovskite cobaltites have attracted significant attention recently due to their intriguing physical properties due to the strong coupling of charge, spin, orbital, and oxygen vacancy interaction in the lattice structures.[1−8] These materials with their tunable multifunctional properties present important application prospects in energy harvesting, sensors, actuators, and new device development based on their ultrafast chemical dynamics nature.[9−11] Among them, double perovskite $LaBaCo_2O_{5.5+\delta}$ (LBCO) is one important family of perovskite cobaltites because of their excellent mixed ionic/electronic conductivity,[12] fascinating strong correlation,[13,14] and anomalous spin-state interactions.[14,15] The epitaxial single-crystalline thin films are highly desired to fully understand and utilize these complex physical phenomena.[16] Liu et al. have investigated the epitaxial nature and interface structures of single-crystalline highly epitaxial $LaBaCo_2O_{5.5+\delta}$ thin films[17] and found that their physical properties have extraordinary sensitivity to the crystal structure, grain orientation, and chemical environment.[12,17,18]

It is widely accepted that the nature of the epitaxial strain state in the thin film has also a great impact on its physical properties.[19,20] For instance, the magnetic and electrical properties in highly epitaxial perovskite thin films are strongly dependent upon the internal strain which results from the lattice mismatch between the film and the substrate.[21−24] Recently, Chen et al. developed a model where the epitaxial nature and physical properties can be tuned by the "local strain" resulting from the surface step dimensions, such as various antiphase domain boundary structures and surface step terrace induced strain.[25−27] It was demonstrated that the microstructure and dielectric properties of $Ba_{0.6}Sr_{0.4}TiO_3$ (BSTO) thin films can be strongly influenced by steps, terraces, and kinks present on the substrate surface.[28,29] Furthermore, they systematically studied the ferromagnetic metallic to ferromagnetic insulator transition by varying the dimension of the surface step terrace induced local domain structures. A four-probe study indicated that the electrical conductivity and metal−insulator transition temperature ($T_{M\text{-}I}$) of the highly epitaxial $La_{0.67}Ca_{0.33}MnO_3$ (LCMO) thin films can be modulated by the dimensions of the surface terraces on MgO (001) miscut substrates.[30]

Investigation of the anisotropic electronic transport properties in highly epitaxial thin films is one of the most effective ways to explore the effects of the local strain induced by the surface step terraces. In this paper, we apply the four-probe scanning tunneling microscopy (4P-STM) technique to study the anisotropic electronic transport phenomena in highly

Received: January 20, 2014
Accepted: April 9, 2014
Published: April 9, 2014

   dx.doi.org/10.1021/am500422j | ACS Appl. Mater. Interfaces 2014, 6, 6704−6708

epitaxial A-site disordered cubic perovskite LBCO thin films on $SrTiO_3$ (STO) (001) vicinal surfaces with different miscut angles. The results show that the anomalous electronic transport properties and the strong anisotropic feature can be tuned by the local strain formed by the substrate step terrace dimensions on the vicinal STO surfaces.

LBCO thin films were epitaxially grown on three different miscut (0.5°, 3.0°, and 5.0°) STO (001) surfaces by using pulsed laser deposition. The optimized condition involves an energy density of about 2.0 J/cm^2 with a laser repetition rate of 5 Hz in an oxygen pressure of 250 mTorr at 850 °C. Processing details can be found in a previous report.[12] Briefly, the as-grown LBCO films were annealed at 850 °C for 15 min in 200 Torr pressure in a pure oxygen atmosphere before being slowly cooled to room temperature at a rate of 5 °C/min. The epitaxial quality and crystallinity of the LBCO films were examined by traditional X-ray diffraction (XRD) (Discover-8) with Cu $K_{\alpha 1}$ radiation. Cross-section transmission electron microscopy (TEM), selected-area electron diffraction (SAED), and high-resolution (HR) TEM analysis were employed to study the epitaxial nature of the film and interface structures. The TEM specimens were prepared by the procedure of mechanical grinding, polishing, and dimpling and ion milling using a Gatan precision ion polishing system (PIPS) equipped with a cold stage. The TEM studies were performed in a Hitachi H-9500 electron microscope operating at 300 keV with point-to-point resolution of 0.18 nm. The resistivity of LBCO thin films was characterized with a square four-probe method in an Omicron ultrahigh vacuum four-probe STM system equipped with a Keithley 4200 apparatus and an in situ scanning electron microscope (SEM).[14] The samples were first annealed at 250 °C for 10 h to desorb water, gases, and other absorptions. The sample temperature was controlled by liquid nitrogen cooling in the range from 130 to 300 K. The four probes are placed in a square shape equally spaced with the distance of 100 μm.

Figure 1 is a typical XRD $\theta-2\theta$ scan of an as-grown LBCO thin film on a 0.5° miscut (001) STO substrate. No significant difference was observed in the patterns with the films grown on the 3.0° and 5.0° miscut surfaces.[29,31] The as-grown films are of a pure LBCO phase with the *c*-axis highly normal to the substrate surface and with only (00*l*) peaks present from the LBCO film overlapped with STO substrate. The rocking curve measurements from the (001) reflections, covering both the film and the substrate together, reveal that the full width at half-maximum (fwhm) is less than 0.1° for all films, as shown in the inset of Figure 1(a), suggesting that the as-grown LBCO films have good single crystallinity and epitaxial quality.

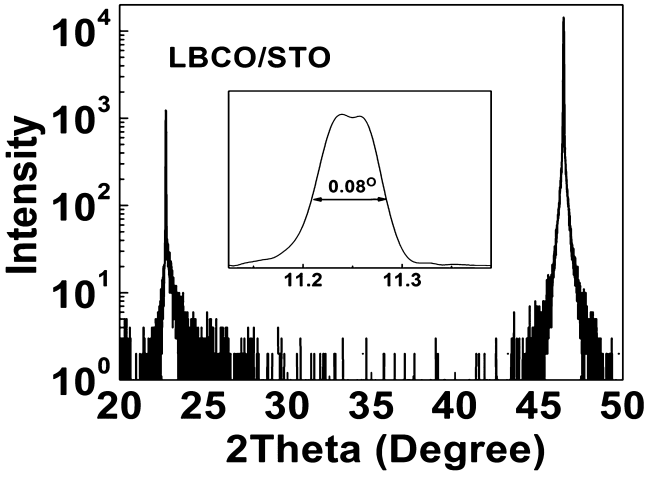

Figure 1. X-ray diffraction pattern obtained from an LBCO thin film on STO (001) substrate with 0.5° miscut angle. All three samples (miscut angles of 0.5°, 3°, and 5°) have similar patterns.

Figure 2 shows the cross-sectional TEM images for the epitaxial LBCO films and their interface structure with respect to the substrate. Figures 2(a), (b), and (c) are cross-section TEM images taken from the LBCO film grown on STO (001) substrate with a miscut angle of 0.5°, 3.0°, and 5.0°, respectively, while the insets are the corresponding SAED patterns. All three films have a uniform thickness of ~80 nm, a flat surface, and a sharp interface with respect to the (001) STO substrate. However, various stripelike structures were found in the different miscut substrates. It is interesting to note that the angles between the stripe lines and the interfaces are equal to the miscut angles. The SAED patterns, shown as insets in Figures 2(a)−(c), were taken from an area covering the entire film and substrate with the electron beam parallel to the $[100]_{STO}$. A single-crystal diffraction pattern of an epitaxial cubic perovskite LBCO film is evident for all three films.[20] It is surprising to observe that no superlattice weak spot associated with the 112-type ordered tetragonal LBCO structure is present in the SAED patterns. Unlike the LBCO films grown on regular (no miscut) substrates,[32] the LBCO films on the vicinal STO surfaces are only the A-site disordered structures or similar to the interlayer of LBCO on STO substrates without a miscut.

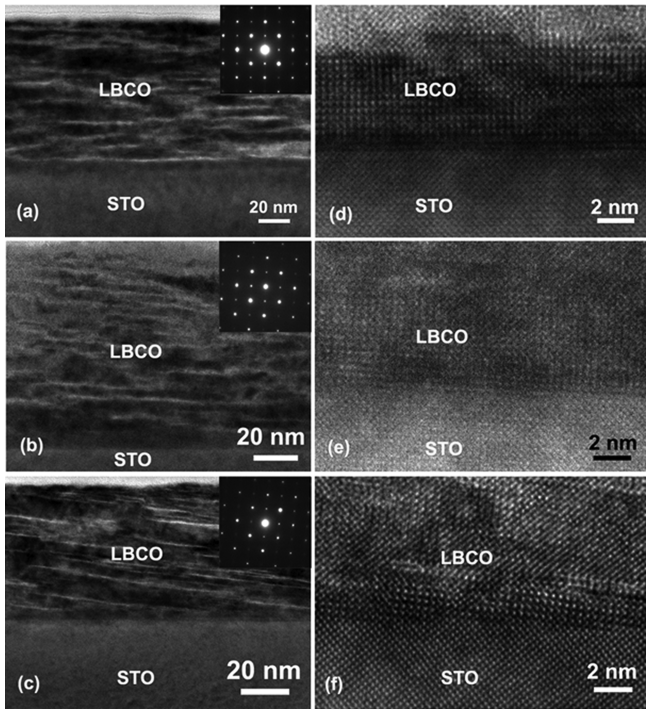

Figure 2. Cross-section TEM image and corresponding SAED (inset) and HRTEM image of the film/substrate interface for the LBCO films grown on STO (001) substrate with miscut angles of 0.5° (a, d), 3.0° (b, e), and 5.0° (c, f).

The mechanism for the formation of an A-site disordered structure could be somewhat related to the interface strain energy accumulation and relaxation. Details are still under

dx.doi.org/10.1021/am500422j | ACS Appl. Mater. Interfaces 2014, 6, 6704−6708

investigation at present and will be reported later. The interface relationships between the LBCO films and STO substrates were determined to be $(001)_{LBCO}//(001)_{STO}$ and $\langle 100\rangle_{LBCO}//\langle 100\rangle_{STO}$ for the miscut samples. Figures 2(d), (e), and (f) show the cross-section HRTEM images of the LBCO/STO interfaces for the films with a miscut angle of 0.5°, 3.0°, and 5.0°, respectively. Clearly, all three LBCO films were well adhered to the STO substrate at the atomic level. However, it can be found, from Figures 2(e) and (f), that the (001) lattice fringes of LBCO are not parallel to the LBCO/STO interface planes and form an angle of 3° and 5°, respectively, with the substrate surface. This feature is in good agreement with the observations of stripes from the low-magnification TEM studies, as shown in Figure 2(a)−(c).

To understand the local strain effect on the electronic transport properties, four-probe STM was employed to carefully study the anisotropic properties of the films on these vicinal STO substrates. The in-plane temperature dependence of the resistivity of the LBCO films on vicinal STO (001) substrates were characterized from 130 to 300 K, as seen in Figures 3(a), (b), and (c). The resistance for all films

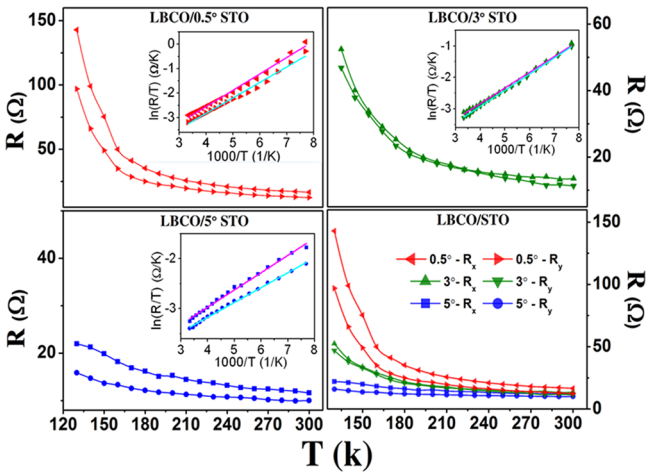

Figure 3. Measured in-plane square resistance−temperature curves from 130 to 300 K of the LBCO films on STO substrates with 0.5°, 3.0°, and 5.0° miscut angles. In (a), (b), and (c), the decrease of resistance $R(T)$ with increasing temperature indicates a typical semiconductor behavior, and the distinct resistance values along the two perpendicular directions (R_x and R_y) show an obvious anisotropic feature in electrical properties of the film. The inset shows the linear fitting of the $\log(R/T)$ to $1/T$ with the small polaron model. (d) Displays the overall results on three miscut substrates.

decreases with increasing temperature, demonstrating that the films have a typical semiconductor behavior in this temperature range.[18,33] However, the in-plane resistance and temperature dependence characteristics vary with the miscut angle. At the low miscut angle of 0.5°, the resistance of LBCO films reveals the highest temperature dependence which is similar to the behavior of the bulk crystal. At a high miscut angle of 5°, the resistance of the film shows much lower temperature dependence. The electronic transport behavior is further analyzed by both the thermal activation model[31] ($\ln R \propto 1/T$) and the small polaron model[34] ($\ln R/T \propto 1/T$). As seen in the inset of Figure 3, the small polaron mechanism shows much better fitting than the thermal activation model, suggesting that in the LBCO thin films the interaction between the electron and lattice is strongly localized. The activation energies E_A of the LBCO films were determined to be 57.5 and 54.4 meV, 44.3 and 43.1 meV, and 29.7 and 25.6 meV on the 0.5°, 3.0°, and 5.0° miscut substrate, respectively.

The strong anisotropic energies and the abnormal transport properties on the miscut substrates can be attributed to the effects from the local strains resulting from the surface step dimensions or the surface step terrace induced strain. The additional strain caused by the different terrace widths on the substrate surface produced by varying the cutting angle has been analyzed in detail previously.[25,35] Generally, there is a residual space (Δd) in each terrace length (d) of the substrate due to the difference in the lattice constant between the epitaxial film and substrate. Considering the real atomic arrangement, the atomic spacing in the film must be tuned to fit the terrace width and eliminate the residual space by generating additional local strain in the different vicinal surfaces. This strain constitutes a main portion of the total strain in the epitaxial thin films and cannot be released by forming misfit dislocations at the interfaces (another portion is the normal strain coming from the lattice misfit between the film and substrate). Therefore, the surface step terrace induced strain is of great importance in affecting the physical properties of the highly epitaxial films.

The miscut (001) $SrTiO_3$ substrate surfaces usually contain various arrays of steps and terraces, depending on the miscut angles. Normally, the (001) $SrTiO_3$ surface consists of surface terraces of various sizes with each step height of one unit cell. Therefore, for the 0.5°, 3.0°, and 5.0° miscut (001) surfaces of $SrTiO_3$, the average widths of the surface terraces can be calculated to be 44.748, 7.458, and 4.474 nm, respectively. The number of unit cells of the substrate $SrTiO_3$ (n_s) that the average terrace can accommodate are 114.60, 19.10, and 11.46, respectively, and accordingly the number of unit cells of LBCO film (n_f) are 115.16, 19.20, and 11.52, respectively. Thus, the difference between n_s and n_f is 0.56, 0.10, and 0.06, respectively. It suggests that the local surface step terrace induced strains for the thin films grown on the 3.0° and 5.0° miscut substrates are very small because of their very slight differences of the n_s and n_f, which also indicate very small residual spaces (Δd). The small lattice-misfit strain and single-domain growth at higher miscut substrates will reduce the scattering of conduction electrons, which leads to a smaller resistance as the film grows on a large miscut angle (001) STO substrate.[30] Thus, the temperature-dependent resistivity of the LBCO films decreases as the miscut angles of the vicinal (001) STO substrates increase as shown in Figure 3(d).

Furthermore, it is important to note that there is a significant difference of the resistance along the two perpendicular directions, R_x and R_y, showing an obvious anisotropic feature in the electrical properties of the LBCO film. This anisotropic phenomenon was not observed in LBCO films grown on the regular (001) STO substrates. However, on the vicinal surface, the residual gap (Δd) gives rise to different mismatches along the a- and b-axis of disorder cubic perovskite LBCO films on cubic STO substrate, which are normal and parallel to the step direction, respectively. Subsequently, the highly epitaxial films on the different step terrace substrates will suffer from different local strains along and perpendicular (x and y) to the surface step terrace edge directions. Thus, a different local strain will become the origin of the anisotropic feature in electrical properties of the LBCO film.

As seen in Figure 3(d), the LBCO film on a 0.5° miscut substrate displays a higher anisotropy in its electrical properties,

dx.doi.org/10.1021/am500422j | ACS Appl. Mater. Interfaces 2014, 6, 6704−6708

while the 3.0° and 5.0° miscut samples show the lower anisotropy of resistances. The magnitude of the anisotropy in resistivity follows the order of the surface step terrace induced local strain. This behavior is consistent with the theoretical analysis based on their average widths, in which the film grown on the 3.0° and 5.0° miscut substrate has the smaller local strain from the surface step compared to that of 0.5° miscut substrates. Furthermore, the resistance variation among various miscut angle (0.5°, 3.0°, or 5.0°) substrates is much higher than that at different (x or y) directions. It should also be noted that the steps on a vicinal substrate will not align perfectly, thus the surface step terrace induced strain only plays an average role in the macroscopic resistance of the epitaxial film. However, it shows clearly that the surface-step terrace effect takes place in this case, and the average terrace widths present with different miscut angles are able to tune the internal strain and the anisotropic resistivity of the LBCO films.

In summary, $LaBaCo_2O_{5.5+\delta}$ thin films were successfully grown by pulsed laser deposition on $SrTiO_3$ (001) vicinal surfaces with different miscut angles. The highly epitaxial LBCO film has a disordered cubic perovskite crystalline structure that is c-axis oriented. The results from the in-plane transport property studies are the first observations of anisotropic resistivity (R_x and R_y) along the two perpendicular directions with a typical semiconductor behavior at low temperature. The anisotropic resistivity characteristics are found to be highly dependent on the miscut angles from 0.5°, 3.0°, and 5.0°. This effect can be attributed to the difference in the film strain resulting from the different terrace widths of the vicinal surfaces. It is reasonable to anticipate that this methodology on a stepped substrate can provide a novel approach to tune the interface structure and physical properties of thin films for functional nanodevices.

■ ASSOCIATED CONTENT

Supporting Information

X-ray diffraction from all vicinal substrates, four-probe electrical transport measurement, transport property analysis with the thermal activation model, and the small polaron model. This material is available free of charge via the Internet at http://pubs.acs.org.

■ AUTHOR INFORMATION

Corresponding Authors

*E-mail: hmguo@iphy.ac.cn.
*E-mail: cl.chen@utsa.edu.

Author Contributions

$^{\perp}$Q.Z. and M.L. have an equal contribution to this research.

Notes

The authors declare no competing financial interest.

■ ACKNOWLEDGMENTS

The work was partially supported by grants from the National Science Foundation of China (No. 61274011, 51210003, 11329402, and 51202185), National "973" projects of China (No. 2013CB932901, 2010CB923004, and 2011CB932700), the Chinese Academy of Sciences, and SSC. It is also partially supported by the US National Science Foundation under NSF-NIRT-0709293 and the Department of Energy under DE-FE0003780.

■ REFERENCES

(1) Tokura, Y.; Nagaosa, N. Orbital Physics in Transition-metal Oxides. *Science* **2000**, *288*, 462−468.
(2) Salamon, M. B.; Jaime, M. The Physics of Manganites: Structure and Transport. *Rev. Mod. Phys.* **2001**, *73*, 583−628.
(3) Luo, G. P.; Wang, Y. S.; Chen, S. Y.; Heilman, A. K.; Chen, C. L.; Chu, C. W.; Liou, Y.; Ming, N. B. Electrical and Magnetic Properties of $La_{0.5}Sr_{0.5}CoO_3$ Thin Films. *Appl. Phys. Lett.* **2000**, *76*, 1908−1910.
(4) Yuan, Z.; Liu, J.; Chen, C. L.; Wang, C. H.; Luo, X. G.; Chen, X. H.; Kim, G. T.; Huang, D. X.; Wang, S. S.; Jacobson, A. J.; Donner, W. Epitaxial Behavior and Transport Properties of $PrBaCo_2O_5$ Thin Films on (001) $SrTiO_3$. *Appl. Phys. Lett.* **2007**, *90*, 212111.
(5) Hayward, M. A.; Rosseinsky, M. J. Anion Vacancy Distribution and Magnetism in the New Reduced Layered Co(II)/Co(I) Phase $LaSrCoO_{3.5-x}$. *Chem. Mater.* **2000**, *12*, 2182−2195.
(6) Vashook, V. V.; Ullmann, H.; Olshevskaya, O. P.; Kulik, V. P.; Lukashevich, V. E.; Kokhanovskij, L. V. Composition and Electrical Conductivity of some Cobaltates of the Type $La_{2-x}Sr_xCoO_{4.5-x/2\pm\delta}$. *Solid State Ionics* **2000**, *138*, 99−104.
(7) Liu, M.; Ma, C.; Liu, J.; Collins, G.; Chen, C.; He, J.; Jiang, J.; Meletis, E. I.; Sun, L.; Jacobson, A. J.; Whangbo, M.-H. Giant Magnetoresistance and Anomalous Magnetic Properties of Highly Epitaxial Ferromagnetic $LaBaCo_2O_{5.5+\delta}$ Thin Films on (001) MgO. *ACS Appl. Mater. Interfaces* **2012**, *4*, 5524−5528.
(8) Ma, C. R.; Liu, M.; Liu, J.; Collins, G.; Zhang, Y. M.; Wang, H. B.; Chen, C. L.; Lin, Y.; He, J.; Jiang, J. C.; Meletis, E. I.; Jacobson, A. J. Interface Effects on the Electronic Transport Properties in Highly Epitaxial $LaBaCo_2O_{5.5+\delta}$ Films. *ACS Appl. Mater. Interfaces* **2014**, *6*, 2540−2545.
(9) Yang, Y. M. L.; Jacobson, A. J.; Chen, C. L.; Luo, G. P.; Ross, K. D.; Chu, C. W. Oxygen Exchange Kinetics on a Highly Oriented $La_{0.5}Sr_{0.5}CoO_{3-\delta}$ Thin Film Prepared by Pulsed-laser Deposition. *Appl. Phys. Lett.* **2001**, *79*, 776−778.
(10) Liu, J.; Collins, G.; Liu, M.; Chen, C. L.; He, J.; Jiang, J. C.; Meletis, E. I. Ultrafast Oxygen Exchange Kinetics on Highly Epitaxial $PrBaCo_2O_{5+\delta}$ Thin Films. *Appl. Phys. Lett.* **2012**, *100*, 024103.
(11) Liu, J.; Collins, G.; Liu, M.; Chen, C. L. Superfast Oxygen Exchange Kinetics on Highly Epitaxial $LaBaCo_2O_{5+\delta}$ Thin Films for Intermediate Temperature Solid Oxide Fuel Cells. *APL Mater.* **2013**, *1*, 3.
(12) Liu, M.; Liu, J.; Collins, G.; Ma, C. R.; Chen, C. L.; He, J.; Jiang, J. C.; Meletis, E. I.; Jacobson, A. J.; Zhang, Q. Y. Magnetic and Transport Properties of Epitaxial $(LaBa)Co_2O_{5.5+\delta}$ Thin Films on (001) $SrTiO_3$. *Appl. Phys. Lett.* **2010**, *96*, 132106.
(13) Fauth, F.; Suard, E.; Caignaert, V. Intermediate Spin State of Co^{3+} and Co^{4+} Ions in $La_{0.5}Ba_{0.5}CoO_3$ Evidenced by Jahn-Teller Distortions. *Phys. Rev. B* **2002**, *65*, 060401(R).
(14) Kundu, A. K.; Rautama, E. L.; Boullay, P.; Caignaert, V.; Pralong, V.; Raveau, B. Spin-locking Effect in the Nanoscale Ordered Perovskite Cobaltite $LaBaCo_2O_6$. *Phys. Rev. B* **2007**, *76*, 184432.
(15) Rautama, E. L.; Boullay, P.; Kundu, A. K.; Caignaert, V.; Pralong, V.; Karppinen, M.; Raveau, B. Cationic Ordering and Microstructural Effects in the Ferromagnetic Perovskite $La_{0.5}Ba_{0.5}CoO_3$: Impact upon Magnetotransport Properties. *Chem. Mater.* **2008**, *20*, 2742−2750.
(16) Jiang, J. C.; Meletis, E. I.; Gnanasekar, K. I. Self-organized, Ordered Array of Coherent Orthogonal Column Nanostructures in Epitaxial $La_{0.8}Sr_{0.2}MnO_3$ Thin Films. *Appl. Phys. Lett.* **2002**, *80*, 4831−4833.
(17) Liu, J.; Collins, G.; Liu, M.; Chen, C. L.; Jiang, J. C.; Meletis, E. I.; Zhang, Q. Y.; Dong, C. A. PO_2 Dependant Resistance Switch Effect in Highly Epitaxial $(LaBa)Co_2O_{5+\delta}$ Thin Films. *Appl. Phys. Lett.* **2010**, *97*, 094101.
(18) Liu, J.; Liu, M.; Collins, G.; Chen, C. L.; Jiang, X. N.; Gong, W. Q.; Jacobson, A. J.; He, J.; Jiang, J. C.; Meletis, E. I. Epitaxial Nature and Transport Properties in $(LaBa)Co_2O_{5+\delta}$ Thin Films. *Chem. Mater.* **2010**, *22*, 799−802.

(19) Rondinelli, J. M.; Spaldin, N. A. Structure and Properties of Functional Oxide Thin Films: Insights from Electronic-Structure Calculations. *Adv. Mater.* **2011**, *23*, 3363−3381.
(20) Liu, M.; Ma, C.; Collins, G.; Liu, J.; Chen, C.; Dai, C.; Lin, Y.; Shui, L.; Xiang, F.; Wang, H.; He, J.; Jiang, J.; Meletis, E. I.; Cole, M. W. Interface Engineered $BaTiO_3/SrTiO_3$ Heterostructures with Optimized High-Frequency Dielectric Properties. *ACS Appl. Mater. Interfaces* **2012**, *4*, 5761−5765.
(21) Schlom, D. G.; Chen, L. Q.; Eom, C. B.; Rabe, K. M.; Streiffer, S. K.; Triscone, J. M. Strain Tuning of Ferroelectric Thin Films. *Annu. Rev. Mater. Res.* **2007**, *37*, 589−626.
(22) Xiong, Y. M.; Chen, T.; Wang, G. Y.; Chen, X. H.; Chen, X.; Chen, C. L. Raman Spectra in Epitaxial Thin Films of $La_{1-x}Ca_xMnO_3$ (x=0.33, 0.5) Grown on Different Substrates. *Phys. Rev. B* **2004**, *70*, 094407.
(23) Xiong, Y. M.; Wang, G. Y.; Luo, X. G.; Wang, C. H.; Chen, X. H.; Chen, X.; Chen, C. L. Magnetotransport Properties in $La_{1-x}Ca_xMnO_3$ (x=0.33, 0.5) Thin Films Deposited on Different Substrates. *J. Appl. Phys.* **2005**, *97*, 083909.
(24) Jiang, J. C.; Henry, L. L.; Gnanasekar, K. I.; Chen, C. L.; Meletis, E. I. Self-assembly of Highly Epitaxial $(La,Sr)MnO_3$ Nanorods on (001) $LaAlO_3$. *Nano Lett.* **2004**, *4*, 741−745.
(25) Lin, Y.; Chen, C. L. Interface Effects on Highly Epitaxial Ferroelectric Thin Films. *J. Mater. Sci.* **2009**, *44*, 5274−5287.
(26) Chen, C. L. *NSF Proposal*, 2002.
(27) Jiang, J. C.; Lin, Y.; Chen, C. L.; Chu, C. W.; Meletis, E. I. Microstructures and Surface Step-induced Antiphase Boundaries in Epitaxial Ferroelectric $Ba_{0.6}Sr_{0.4}TiO_3$ Thin Film on MgO. *J. Appl. Phys.* **2002**, *91*, 3188−3192.
(28) Liu, S. W.; Weaver, J.; Yuan, Z.; Donner, W.; Chen, C. L.; Jiang, J. C.; Meletis, E. I.; Chang, W.; Kirchoefer, S. W.; Horwitz, J.; Bhalla, A., Ferroelectric $(Pb,Sr)TiO_3$ Epitaxial Thin Films on (001) MgO for Room Temperature High-frequency Tunable Microwave Elements. *Appl. Phys. Lett.* **2005**, *87*.
(29) Chen, C. L.; Shen, J.; Chen, S. Y.; Luo, G. P.; Chu, C. W.; Miranda, F. A.; Van Keuls, F. W.; Jiang, J. C.; Meletis, E. I.; Chang, H. Y. Epitaxial Growth of Dielectric $Ba_{0.6}Sr_{0.4}TiO_3$ Thin Film on MgO for Room Temperature Microwave Phase Shifters. *Appl. Phys. Lett.* **2001**, *78*, 652−654.
(30) Lu, H. L.; Zhang, C. D.; Guo, H. M.; Gao, H. J.; Liu, M.; Liu, J. A.; Collins, G.; Chen, C. L. Surface-Step-Terrace-Induced Anomalous Transport Properties in Highly Epitaxial $La_{0.67}Ca_{0.33}MnO_3$ Thin Films. *ACS Appl. Mater. Interfaces* **2010**, *2*, 2496−2499.
(31) Ma, C. R.; Liu, M.; Collins, G.; Wang, H. B.; Bao, S. Y.; Xu, X.; Enriquez, E.; Chen, C. L.; Lin, Y.; Whangbo, M. H. Magnetic and Electrical Transport Properties of $LaBaCo_2O_{5.5+\delta}$ Thin Films on Vicinal (001) $SrTiO_3$ Surfaces. *ACS Appl. Mater. Interfaces* **2013**, *5*, 451−455.
(32) He, J.; Jiang, J. C.; Liu, J.; Liu, M.; Collins, G.; Ma, C. R.; Chen, C. L.; Meletis, E. I. Self-patterned Nano Structures in Structurally Gradient Epitaxial La0.5Ba0.5CoO3 Films. *Thin Solid Films* **2011**, *519*, 4371−4376.
(33) Kundu, A. K.; Raveau, B.; Caignaert, V.; Rautama, E. L.; Pralong, V. Electron Transport and Thermoelectric Properties of Layered Perovskite $LaBaCo_2O_{5.5}$. *J. Phys.: Condens. Matter* **2009**, *21*, 056007.
(34) Iguchi, E.; Ueda, K.; Jung, W. H. Conduction in $LaCoO_3$ by Small-polaron Hopping below Room Temperature. *Phys. Rev. B* **1996**, *54*, 17431−17437.
(35) Ma, C. R.; Liu, M.; Chen, C. L.; Lin, Y.; Li, Y. R.; Horwitz, J. S.; Jiang, J. C.; Meletis, E. I.; Zhang, Q. Y. The Origin of Local Strain in Highly Epitaxial Oxide Thin Films. *Sci. Rep.* **2013**, *3*, 3092.